ELSEVIER

Journal of Chromatography A, 959 (2002) 229–239

JOURNAL OF CHROMATOGRAPHY A

www.elsevier.com/locate/chroma

Electromigration dispersion in capillary zone electrophoresis Experimental validation of use of the Haarhoff–Van der Linde function

Guillaume L. Erny, Edmund T. Bergström, David M. Goodall*

Department of Chemistry, University of York, York YO10 5DD, UK

Received 3 January 2002; received in revised form 2 April 2002; accepted 11 April 2002

Abstract

This paper provides experimental validation of the use of the Haarhoff–Van der Linde (HVL) peak fitting function to fit experimental capillary zone electrophoresis (CZE) electropherograms. The test mixtures were composed of paraquat over a five order of magnitude concentration range (1.2 μ*M* to 120 m*M*) and 4-aminopyridine at constant concentration (0.53 m*M*) as internal standard. Peak descriptors and electrophoresis parameters were extracted reliably by a Gaussian function from 4 to 40 μ*M*; by the HVL function from 120 μ*M* to 4 m*M*; and by a triangular function from 4 to 120 m*M*. The HVL function can be used where there is significant peak asymmetry due to electromigration distortion (EMD) and the Gaussian contribution toward the peak variance is greater than 25%. The peak centre (a_1) and the Gaussian variance (a_2) of the paraquat peak are shown to be independent of concentration. Diffusion coefficients obtained from a_2 for both analytes were found to be in good agreement with their theoretical values. For all peaks where the distortion coefficient (a_3) can be extracted, this parameter is shown to be directly proportional to the sample loading, as predicted by EMD theory. For the 4-aminopyridinium ion, mobilities calculated from a_3 and measured independently are in excellent agreement. These results show that the HVL function accurately describes the two major processes, diffusion and EMD, contributing to the variance during a CZE separation.

Keywords: Dispersion; Validation; Haarhoff–Van der Linde function; Peak shape; Paraquat; Aminopyridines; Pesticides; Pyridines

1. Introduction and theory

In a recent publication [1], we showed theoretically and using simulations of model separations that CZE peaks distorted by electromigration dispersion (EMD) could accurately be fitted with the Haarhoff–Van der Linde (HVL) function [2], which is given by

$$f(x) = \frac{\frac{a_0 a_2}{a_1 a_3 \sqrt{2\pi}} \cdot \exp\left[-\frac{1}{2}\left(\frac{x-a_1}{a_2}\right)^2 \right]}{\frac{1}{\exp\left(\frac{a_1 a_3}{a_2^2}\right) - 1} + \frac{1}{2} \cdot \left[1 + \mathrm{erf}\left(\frac{x-a_1}{\sqrt{2}a_2}\right) \right]} \quad (1)$$

*Corresponding author. Tel.: +44-1904-432-574; fax: +44-1904-432-516.

E-mail address: dmg1@york.ac.uk (D.M. Goodall).

0021-9673/02/$ – see front matter
PII: S0021-9673(02)00454-5

where a_0 is the peak area, a_1 and a_2 are the peak centre and the standard deviation of the Gaussian part, respectively, and a_3 is the peak distortion: x is either time or distance, and the units of the various a parameters are consistent with this. Initially designed for overloaded gas chromatographic peaks, this function can be seen as a mix between a Gaussian and a triangular function, the Gaussian component being related to diffusional processes, and the triangular component to electromigration dispersion. All parameters can be predicted using the equations for electrophoretic transport [3], diffusion [4], and electromigration dispersion [3,5,6] as follows. For the peak centre in time units

$$a_1 = \frac{lL}{\mu_A^{app} V} \tag{2}$$

where l, L, μ_A^{app}, and V are the length from injection to detection, the total capillary length, the apparent mobility of the analyte and the applied voltage, respectively.

For the Gaussian variance in distance units

$$a_2^2 = 2D_A t_D + \frac{l_0'^2}{12} \tag{3}$$

where D_A is the analyte diffusion coefficient, t_D the time from injection to detection, and l_0' the effective injection length, i.e. the injection length after stacking or destacking. Eq. (3) assumes diffusion and injection as the only sources of symmetric variance [4].

For the peak distortion in distance units

$$a_3 = -2z_A A_A c_A^I l_0 \tag{4}$$

where z_A, c_A^I and l_0 are the charge of the analyte, the analyte concentration in the injection zone, and the injection length, respectively. A_A is a constant dependent on the starting conditions. In the case of a 1:1 background electrolyte (BGE) constituted of fully charged ions, A_A has been shown by Mikkers to be given by [6]

$$A_A = -\frac{(\mu_A - \mu_{co})(\mu_A - \mu_{counter})}{c_{co}^B \mu_A (\mu_{co} - \mu_{counter})} \tag{5}$$

where μ_A, μ_{co} and $\mu_{counter}$ are the mobilities of the analyte, its co-ion and counter-ion, respectively, and c_{co}^B is the co-ion concentration in the BGE.

To ensure compatibility with Eq. (1), all parameters calculated from Eqs. (2)−(4) need to be in the same units; they can be converted from time (s) to distance (m) using

$$\begin{aligned} a_i(\mathrm{m}) &= \frac{a_i(\mathrm{s})}{M_1} \cdot l; (i = 1,2) \\ a_3(\mathrm{m}) &= -\frac{a_3(\mathrm{s})}{M_1} \cdot l \end{aligned} \tag{6}$$

where M_1 is the first moment of the peak, defined as [7]

$$M_1 = \frac{1}{a_0} \int_0^\infty f(x) x \, dx \tag{7}$$

and has the same dimensions as x, which is defined along with $f(x)$ in Eq. (1).

The total variance of the HVL peak has been shown to be a combination of the variance due to diffusion and the variance due to electromigration dispersion. It is not the summation of both variances, but can be calculated using the universal function [1]

$$\frac{M_2}{a_2^2} = 6.115 - 1.523 \times 10^{-1} G + 1.524 \times 10^{-3} G^2 - 5.12 \times 10^{-6} G^3 \tag{8}$$

where M_2 is the second moment of the peak (total peak variance), and G the percentage of Gaussian variance defined as follows

$$G = \frac{a_2^2}{a_2^2 + \frac{1}{9} a_1 |a_3|} \times 100 \tag{9}$$

Using the same approach as has been used for setting the limit for extra-column dispersion in LC [8], which is that in order not to spoil the resolution, the extra-column variance should be no more than 10% of the column variance, we have previously given an equation that may be used to determine the value of G at this point [1].

In our previous paper, we only used simulated peaks. In this paper, the aim is to study the quality of the fit in a real system, and the reliability of the extracted parameters at different degrees of peak distortion. The test compound is the cationic herbicide paraquat (1,1′-dimethyl-4,4′-bipyridinium), and its concentration is varied from 1.2 μM to 120

m*M*. 4-Aminopyridine is used as an internal standard at a concentration of 0.53 m*M*.

2. Experimental

2.1. Apparatus

The laboratory-made CE apparatus used has been described elsewhere [9]. Detection was by UV absorbance, using a fibre-optic bundle to couple the output from a 30 W deuterium lamp through an 11.4-mm long detection zone on the capillary. An imaging grating formed a wavelength resolved image of the detection zone on a CCD chip. The CCD camera provides a series of snapshot images of the analyte bands migrating through the detection zone, and these data are processed to produce the electropherograms [9,10]. The capillaries used were polyimide coated, fused-silica 75 μm I.D.×363 μm O.D. (Composite Metals, Hallow, UK), 500 mm long and 400 mm to the end of the detection zone. Sample injection was performed hydrodynamically and timed manually: for example, with the sample vial level held 10 mm higher than the output vial level for 46 s, a 7-nl volume was injected. The experiments necessary to calculate the mobility of 4-aminopyridine were performed on a Beckman CE instrument (Beckman P/ACE 2050 with System Gold software, Beckman, High Wycombe, UK). The capillaries used were 50 μm I.D. 470 mm long and 400 mm to the end of the detection zone.

2.2. Peak fitting software

Fitting of the peaks was carried out using commercial peak analysis software (PeakFit version 4, SPSS, Chicago, USA). The fitting software allows three different methods for peak detection and fitting; a residual, a second derivative and a deconvolution method (methods I, II and III, respectively). These methods are used to automatically detect hidden peaks, with the fitting algorithms the same in all methods. As there are no hidden peaks in our electropherograms, method I was used in all experiments. Once the method is selected, the software allows different choices of smoothing and baseline subtraction. By fitting a function to a chromatogram, the results for the extracted parameters should be independent of the background noise, provided that the peak is high enough to be detected. No data smoothing was used in the fitting. The baseline is one of the most important features to control to obtain reliable extracted parameters. A large choice of baseline functions is available; constant, linear, quadratic, cubic logarithmic, etc. The algorithms will fit the baseline as well as the chromatographic function, and the software can automatically select the best-fit baseline. Regression analysis was carried out using the program SPSS (SPSS version 10, SPSS).

2.3. Materials

The acetate buffer used for all separations on the laboratory-made CE apparatus was made by adjusting 50 m*M* sodium acetate (Fisons, Loughborough, UK) to pH 4.6 with glacial acetic acid (Fisher Scientific, Loughborough, UK). Sodium hydroxide and hydrochloric acid (Fisher Scientific, Loughborough, UK) were used for capillary conditioning. The capillary was initially conditioned with 0.1 *M* NaOH solution, and during the series of experiments reported in this paper was rinsed for 2 min with 0.5 *M* HCl followed by a 2-min rinse with the acetate buffer background electrolyte (BGE). The analyte samples were 4-aminopyridine (Sigma, Gillingham, UK) and a dry paraquat dichloride sample (Syngenta, Jealotts Hill, UK). The sample was prepared in 20% BGE [11]. All solutions were made up using purified water (Elgastat UHQII, Elga, High Wycombe, UK).

3. Results and discussion

Two separations were carried out for each concentration of paraquat. The concentration of the aminopyridine used as an internal standard remaining constant and equal to 0.53 m*M*. Under the conditions of the experiments, aminopyridine is present as its conjugate acid, the aminopyridinium cation. Symbols used for the cationic species aminopyridinium and paraquat are AP and PQ, respectively. Electropherograms are shown in Fig. 1 for PQ concentrations of 4 μ*M* and 4 m*M*. Peak heights for PQ

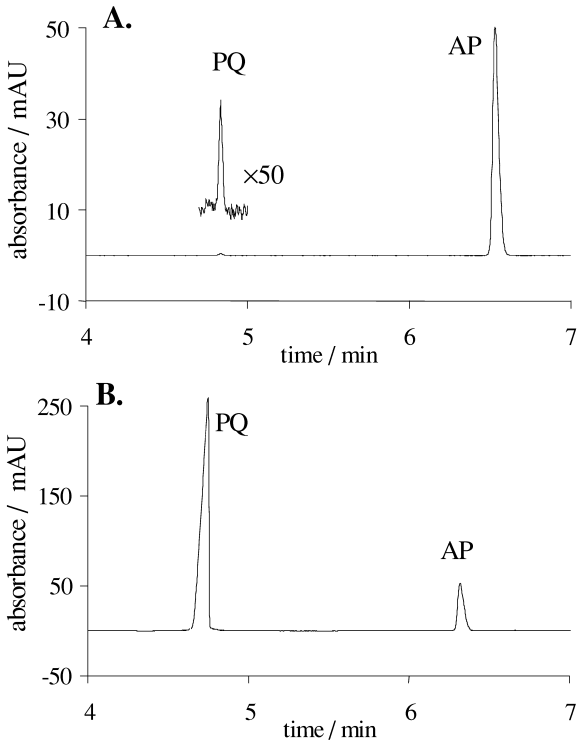

Fig. 1. Electropherograms obtained with a BGE constituted of 50 m*M* sodium acetate adjusted to pH 4.6 with acetic acid. Running voltage, 10 kV; capillary length 50 mm, 40 mm to detector. Injection of ~10 nl sample containing 0.53 m*M* of 4-aminopyridine with (A), 4 μ*M* and (B), 4 m*M* of paraquat dichloride.

are seen to increase from ~400 μAU to 250 mAU on increasing the concentration by a factor 1000. If there were no EMD, an increase by a factor of 1000 in peak height would be expected. The presence of EMD is evident from appreciable peak fronting for PQ at a concentration of 4 m*M*. The AP peak shows tailing. An important feature of the CCD detection scheme used is that part of the image is used for baseline correction, which leads to a very good baseline.

Three different functions have been used to fit the experimental data: a Gaussian function of area a_0, peak centre a_1 and standard deviation a_2; the HVL function; and a triangular function of area a_0 and peak width at base $\sqrt{2a_1|a_3|}$. The triangular and Gaussian functions have been shown to be the limits of the HVL function when the distortion coefficient (a_3) and the standard deviation (a_2), respectively

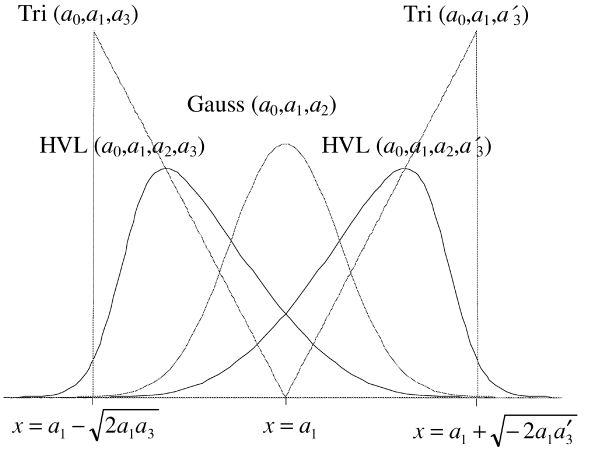

Fig. 2. Triangular, Gaussian and HVL peak shapes for $a_0 = 1$, $a_1 = 5$, $a_2 = 0.5$, $a_3 = 0.3$ and $a'_3 = -0.3$.

tend to zero [1]. The three functions are compared in Fig. 2 for illustrative values of the various parameters. Peak tailing in the distance domain corresponds to a positive value of a_3, and tailing to a negative value of a_3. The reverse is true in the time domain (cf. Eq. (6)).

3.1. Quality of the fitting

Fig. 3 shows the experimental data points and the fitted function at PQ concentrations of: (a) 4 μ*M*, (b) 400 μ*M* and (c) 4 m*M*, together with the corresponding percentage residual, RES, defined as

$$\mathrm{RES} = \frac{A_{\mathrm{exp}} - A_{\mathrm{HVL}}}{A_{\mathrm{exp}}^{\mathrm{max}}} \times 100 \qquad (10)$$

where A_{exp}, A_{HVL} and $A_{\mathrm{exp}}^{\mathrm{max}}$ are the experimental absorbance data point, the theoretical absorbance from the fitted HVL function at this point, and the absorbance at the peak maximum, respectively. At 4 μ*M*, the signal-to-RMS noise ratio is equal to 10, all the percentage residual originates from the noise, and a perfect fitting was obtained. At 400 μ*M*, the baseline noise is negligible in comparison to the peak height. The fitting is very good, with a percentage residual never greater than 0.8%. At 4 m*M*, the fitting starts to deteriorate, with the percentage residual reaching −1.3% at one point. This is due to numerical limitations of the fitting software when

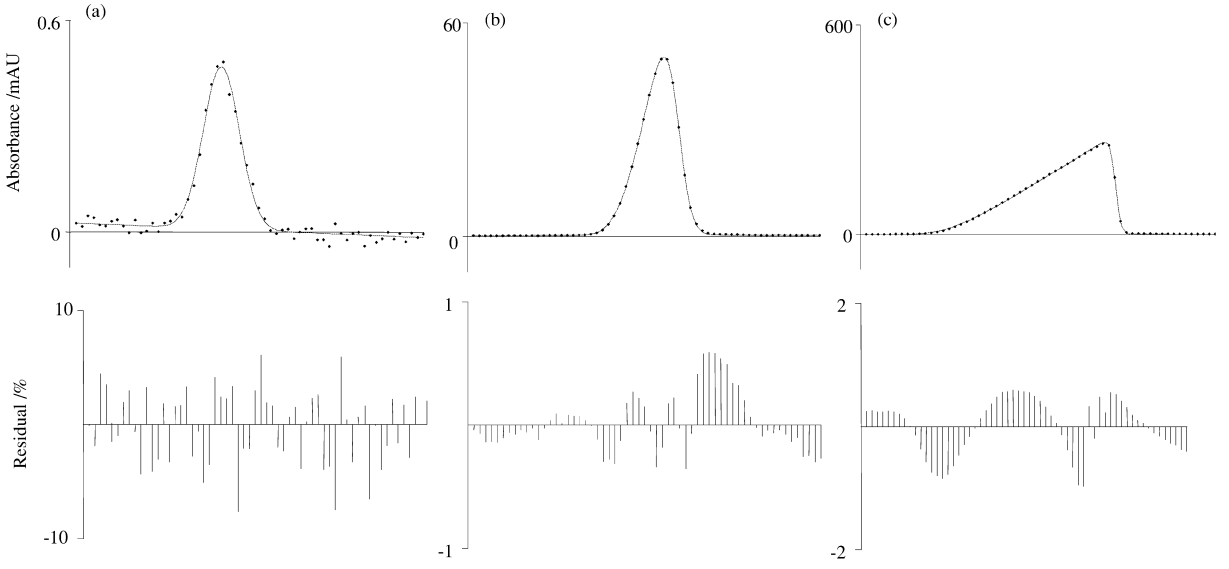

Fig. 3. Fitting with the HVL model of experimental electropherograms and percentage residual, at three different PQ concentrations, (a) 4 μ*M*, (b) 400 μ*M* and (c) 4 m*M*.

evaluating the HVL function, particularly for highly distorted peaks when a_3 is negative. In the case for the 4 m*M* PQ peak, the first term of the denominator of Eq. (1) is $1/[\exp(-31.6)-1.0]$: the limited arithmetic precision leads to inaccuracy when subtracting 1.0 from a very small number. This inaccuracy becomes significant for the function as a whole when the value of the second term in the denominator approaches 1.0 and the denominator becomes very small: at peak maximum the second term is equal to $1.0-2\times10^{-13}$. From 4 to 400 μ*M*, the peak height scales with the concentration (~0.5 mAU at 4 μ*M* PQ, ~50 mAU at 400 μ*M*). A strong distortion is observed at 4 m*M*, and the peak height is half the value expected if there were no EMD. At 4 m*M* PQ, the analyte concentration is above the value where EMD degrades the peak efficiency by less than 10% [1]. At higher concentrations the triangular function has to be used, and Fig. 4 shows data points from 12 m*M* PQ fitted in this way. At even higher PQ concentrations (over 12 m*M*), the AP and PQ peaks show a new type of distortion as shown in Fig. 5; this is believed to be due to the influence of the injection length. The sample is injected in 20% BGE/80% water. At low sample concentration, the electric field in the injection zone will be higher than in the BGE zone, stacking will occur and the effective injection length will decrease by roughly a factor of five [11]. When the concentration of PQ is increased, the electric field in the injection zone decreases, and the stacking effect decreases. At very high sample concentration (40 and 120 m*M* PQ), the contribution to the conductivity from the injected PQ (charge 2+) is higher than that from the co-ion in the BGE zone (50 m*M* Na^+). Consequently, the electric field in the injection zone will be lower than in the sample zone, destacking will occur, and the rectangular peak shape from

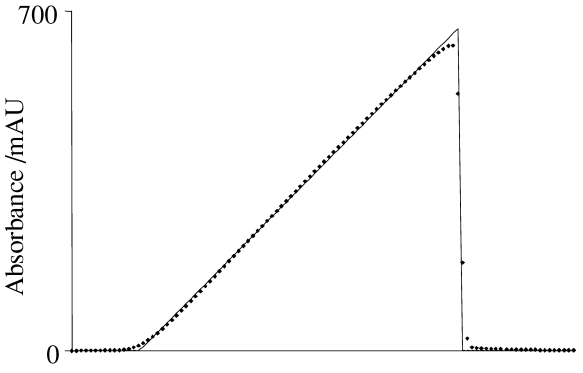

Fig. 4. Experimental data points at a PQ concentration of 12 m*M* and fitting with the triangular function.

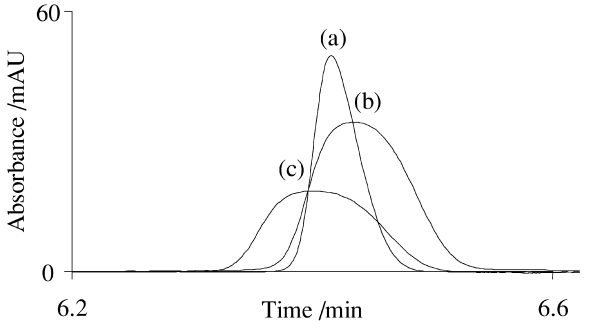

Fig. 5. AP peak shapes at injected concentration of PQ equal to (a) 12 m*M*, (b) 40 m*M*, and (c) 120 m*M*.

the injection plug can still be observed in the peak shape after migration to the detector.

3.2. 4-Aminopyridine peak

In our initial publication on the application of CCD-based absorbance detection to CE analysis of paraquat and related species, 4-aminopyridine was used as an internal standard to calculate the actual volume injected [12]. To do this, the system's response for AP, R_{AP}, was measured by filling the capillary with a solution of 0.5 m*M* aminopyridine in the BGE and found to be $R_{AP}=0.112$ AU m^3 mol^{-1}. The injection length, l_0, can be calculated using the normalised area, A_{norm} (AU)

$$l_0 = \frac{A_{norm} l}{c^{I}_{AP} R_{AP}} \tag{11}$$

where c^{I}_{AP} is the injected aminopyridine concentration, and l the length from injection to detection.

Each data set has been fitted with the HVL model, and the four HVL parameters extracted, as well as the first moment, the second moment and the peak maximum. From these parameters the normalised area, A_{norm}, was calculated using

$$A_{norm} = \frac{a_0}{M_1} \tag{12}$$

where M_1 is the first moment of the peak. The peak standard deviation, a_2, and the peak distortion coefficient, a_3, were converted to distance units using Eq. (6), and the efficiency, N, was calculated using the equation

$$N = \frac{M_1^2}{M_2} \tag{13}$$

Results are presented in Table 1.

For concentrations of PQ greater than 12 m*M* in the injection zone, the AP peak could not be fitted by the HVL model due to the distortion from the rectangular injection plug, as discussed in Section 3.1. Without the influence of the rectangular plug, all extracted parameters from the AP peak should be constant. The normalised area was found to be $(3.7\pm0.8)\times10^{-4}$ AU; the high RSD (22%) is due to the way injection is done in the laboratory-made CE apparatus, leading to poor reproducibility of the injection length. The average value of a_3 from Table 1 is $(11.3\pm2.6)\times10^{-6}$ m. As a_3 is proportional to the sample loading, the same variation as for the peak area is expected and indeed found (RSD in $a_3=23\%$). In Fig. 6, a_3 is plotted as a function of the injection length calculated from the normalised area using Eq. (11). The very good linearity observed in this figure, with RSD on the slope less than 2%, shows that the distortion coefficient may be reliability extracted by the HVL fitting.

To check consistency with the Mikkers' equation (Eq. (4)), the value of A_A was calculated from the slope in Fig. 6 to be (-4.76 ± 0.07) dm^3 mol^{-1} and used to estimate the mobility of AP. Using Eq. (5) and the values of 5.19 and -4.27×10^{-8} m^2 V^{-1} s^{-1} for the ionic mobilities at 298 K and zero ionic strength, μ^o, of the sodium and acetate ions, respectively [13], the mobility of the aminopyridinium ion under the same conditions was calculated to be $(4.09\pm0.06)\times10^{-8}$ m^2 V^{-1} s^{-1}. The AP mobility was independently measured in a BGE comprising 20 m*M* sodium acetate adjusted to pH 4.6 with acetic acid using a Beckman CE apparatus with capillary thermostatted at 298 K, and corrected to zero ionic strength using the equation from Survay et al. [14]. The resulting value of $\mu^o=(3.98\pm0.01)\times10^{-8}$ m^2 V^{-1} s^{-1} (μ at 20 m$M=(3.50\pm0.01)\times10^{-8}$ m^2 V^{-1} s^{-1}) is in very good agreement with value estimated using A_A.

The diffusion coefficient, D_A, extracted from the Gaussian variance using Eq. (3) and corrected to the ionic strength of the experiment [15] was found equal to $(1.39\pm0.03)\times10^{-9}$ m^2 s^{-1}. The effective injection length was estimated to be one-fifth of the

Table 1
Parameters extracted with HVL fitting of the AP peak for different injected concentrations of PQ

[Paraquat] (M)	A_{norm} (AU)	a_1 (s)	a_2 (10^{-3} m)	a_3 (10^{-6} m)	G (%)	N (10^4)
1.2×10^{-6}	3.46×10^{-4}	386	1.06	10.5	70.7	12.3
1.2×10^{-6}	3.40×10^{-4}	385	1.07	10.3	71.2	12.3
4.0×10^{-6}	3.48×10^{-4}	394	1.06	10.4	70.8	12.4
4.0×10^{-6}	3.53×10^{-4}	392	1.07	10.5	70.6	12.3
1.2×10^{-5}	3.33×10^{-4}	385	1.06	10.0	71.6	12.5
1.2×10^{-5}	3.21×10^{-4}	383	1.06	9.6	72.5	12.5
4.0×10^{-5}	3.33×10^{-4}	390	1.06	9.9	71.8	12.5
4.0×10^{-5}	3.47×10^{-4}	388	1.06	10.3	70.9	12.4
1.2×10^{-4}	3.69×10^{-4}	383	1.06	11.0	69.8	12.1
1.2×10^{-4}	3.61×10^{-4}	382	1.06	10.8	70.1	12.2
4.0×10^{-4}	3.49×10^{-4}	400	1.07	10.3	70.8	12.5
4.0×10^{-4}	3.61×10^{-4}	394	1.06	11.1	69.9	12.1
1.2×10^{-3}	3.60×10^{-4}	381	1.05	10.9	70.2	12.0
1.2×10^{-3}	3.07×10^{-4}	380	1.06	9.4	73.2	12.5
4.0×10^{-3}	3.77×10^{-4}	380	1.07	11.5	69.4	11.7
4.0×10^{-3}	3.63×10^{-4}	389	1.07	10.9	70.6	11.8
1.2×10^{-2}	6.30×10^{-4}	397	1.14	19.8	59.6	9.0
1.2×10^{-2}	5.09×10^{-4}	397	1.12	16.3	63.6	9.9
4.0×10^{-2}	5.11×10^{-4}	NA	NA	NA	NA	NA
4.0×10^{-2}	4.37×10^{-4}	NA	NA	NA	NA	NA
1.2×10^{-1}	3.01×10^{-4}	NA	NA	NA	NA	NA
1.2×10^{-1}	3.84×10^{-4}	NA	NA	NA	NA	NA

NA, not applicable.

injection length; this accounts for stacking, since the sample is injected in 20% BGE solution [4]. The time between injection and the start of the separation was 30 s. For small ions, the diffusion coefficient can be estimated by [15]

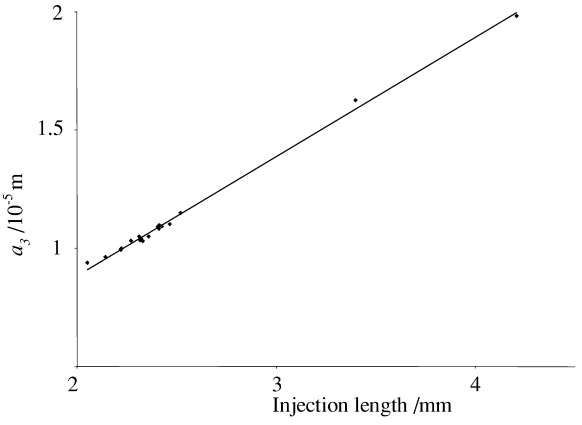

Fig. 6. Dependence on injection length of a_3 extracted from the HVL function for the aminopyridinium peak.

$$D_A^0 = \frac{\mu_A^0 kT}{z_A e} \quad (14)$$

where μ_A^0 is the mobility at zero ionic strength and at the temperature of the experiment, T the absolute temperature, z_A the analyte charge number, e the electronic charge, and k the Boltzmann constant. In our unthermostatted instrument, with a voltage of 10 kV and a current of 43 μA, the temperature rise inside the capillary was estimated to be 12 K [16], leading to a temperature inside the capillary of 306 K. The value of the mobility at 306 K can be calculated from its measured value at 298 K using Eq. (15) [17]

$$\mu^0(306\,\mathrm{K}) = \frac{\eta_{298}}{\eta_{306}} \cdot \mu^0\ (298\,\mathrm{K}) \quad (15)$$

where η_T is the viscosity of water at the temperature T [18]. Using Eq. (14) and 4.72×10^{-8} m^2 V^{-1} s^{-1} for the mobility of AP at 306 K, the diffusion coefficient was estimated to be 1.25×10^{-9} m^2 s^{-1}. Considering the different potential sources of uncer-

tainty (effective injection length, temperature inside the capillary, analyte mobility), this value is in good agreement with the measured value of $(1.39\pm0.03)\times10^{-9}$ m^2 s^{-1} at the temperature of the experiment.

The good agreement between experimental and theoretical values for A_A and D_A provides unambiguous validation of the use of the HVL model in fitting CZE peaks, and shows the power of the combination of Mikkers theory and HVL peak parameterisation. Our results suggest that in cases where an ionic mobility cannot be measured directly, it may be readily obtained from measurement of the peak distortion coefficient.

The average efficiency, N, is calculated from Table 1 to be $(12\pm1)\times10^4$. As the Gaussian efficiency, given by a_1^2/a_2^2, equals $(14.0\pm0.6)\times10^4$, it follows that EMD decreases the efficiency of the AP peak by 15%.

3.3. Paraquat peak

For the paraquat (PQ) peak, results obtained using the three fitting functions are presented in Table 2. The Gaussian fitting was applicable from 1.2 to 40 μM, the HVL from 40 μM to 4 mM and the triangular fitting from 4 to 120 mM. Outside these ranges, the functions were not applicable (abbreviation NA in the table). In combination, the three functions cover the whole five orders of magnitude dynamic range of the experiment. Because of signal-to-noise considerations at the lowest concentration (1.2 μM), the Gaussian fitting does not reliably extract all peak parameters, as can be seen by the value of a_2 at this concentration which is significantly higher than values over the range 40–400 μM. From 40 μM to 1.2 mM, the HVL fitting is successful in separating diffusion from EMD. This is shown by the constant value of a_2 [$a_2=(0.821\pm0.019)\times$

Table 2
Parameters extracted with the HVL, Gaussian and triangular fitting of the PQ peak over a five orders of magnitude range of concentrations

[Paraquat] (M)	l_0 (10^{-3} m)	Gaussian fitting			HVL fitting				Triangular fitting			G (%)	N (10^4)
		A_{norm} (AU)	a_1 (s)	a_2 (10^{-3} m)	A_{norm} AU	a_1 (s)	a_2 (10^{-3} m)	a_3 (10^{-6} m)	A_{norm} AU	a_1 (s)	a_3 (10^{-6} m)		
1.2×10^{-6}	2.31	6.84×10^{-7}	285	1.01	NA	NA	NA	NA	NA	NA	NA	100	15.6
1.2×10^{-6}	2.27	6.30×10^{-7}	284	0.917	NA	NA	NA	NA	NA	NA	NA	100	19.0
4.0×10^{-6}	2.33	2.46×10^{-6}	290	0.816	NA	NA	NA	NA	NA	NA	NA	100	24.0
4.0×10^{-6}	2.36	2.45×10^{-6}	290	0.803	NA	NA	NA	NA	NA	NA	NA	100	24.8
1.2×10^{-5}	2.22	7.50×10^{-6}	284	0.816	NA	NA	NA	NA	NA	NA	NA	100	24.0
1.2×10^{-5}	2.14	6.93×10^{-6}	283	0.816	NA	NA	NA	NA	NA	NA	NA	100	24.1
4.0×10^{-5}	2.22	2.41×10^{-5}	287	0.807	2.42×10^{-5}	287	0.810	0.31	NA	NA	NA	97.9[a]	24.4[a]
4.0×10^{-5}	2.32	2.55×10^{-5}	286	0.812	2.54×10^{-5}	286	0.816	0.11	NA	NA	NA	99.3[a]	24.0[a]
1.2×10^{-4}	2.47	NA	NA	NA	8.54×10^{-5}	283	0.817	−1.61	NA	NA	NA	90.3	23.7
1.2×10^{-4}	2.41	NA	NA	NA	8.29×10^{-5}	282	0.815	−1.52	NA	NA	NA	90.8	23.8
4.0×10^{-4}	2.33	NA	NA	NA	2.71×10^{-4}	295	0.823	−6.15	NA	NA	NA	71.3	20.6
4.0×10^{-4}	2.41	NA	NA	NA	2.80×10^{-4}	290	0.831	−6.46	NA	NA	NA	70.7	20.1
1.2×10^{-3}	2.41	NA	NA	NA	8.70×10^{-4}	281	0.856	−22.0	NA	NA	NA	43.0	10.9
1.2×10^{-3}	2.05	NA	NA	NA	7.43×10^{-4}	280	0.848	−18.7	NA	NA	NA	46.5	12.2
4.0×10^{-3}	2.52	NA	NA	NA	2.90×10^{-3}	280	0.982	−76.9	2.87×10^{-3}	279	−89	22.2[a]	5.7[a]
4.0×10^{-3}	2.43	NA	NA	NA	2.73×10^{-3}	286	0.961	−71.2	2.76×10^{-3}	286	−83	22.8[a]	3.8[a]
1.2×10^{-2}	4.21	NA	NA	NA	NA	NA	NA	NA	1.50×10^{-2}	291	−425	0	0.8
1.2×10^{-2}	3.40	NA	NA	NA	NA	NA	NA	NA	1.22×10^{-2}	290	−356	0	1.0
4.0×10^{-2}	3.41	NA	NA	NA	NA	NA	NA	NA	3.42×10^{-2}	282	−896	0	0.4
4.0×10^{-2}	2.92	NA	NA	NA	NA	NA	NA	NA	3.22×10^{-2}	280	−902	0	0.4
1.2×10^{-1}	2.01	NA	NA	NA	NA	NA	NA	NA	6.84×10^{-2}	278	−1890	0	0.2
1.2×10^{-1}	2.56	NA	NA	NA	NA	NA	NA	NA	8.77×10^{-2}	279	−2340	0	0.2

NA, not applicable.
[a] Values calculated with the results of the HVL fitting.

10^{-3} m], independent of the degree of peak distortion. *G* goes from 99 to ~45%, accompanied by a decrease in efficiency from 24 to 12×10^{4}. In parallel, above 40 μ*M*, the HVL function successfully extracts a distortion coefficient which is linear with sample loading, as predicted by theory on EMD. At 4 m*M*, the HVL fitting starts to deteriorate, this can be noticed by the increase in a_2, and the triangular function was used to extract a value of a_3 at this and higher concentrations. With this function, a_2 is assumed negligible, so the fitting is particularly good at very high loading.

In our previous paper on the HVL function, simulations showed that use of a_1 gave mobilities which were constant even when peaks were heavily distorted, whereas mobilities calculated using the migration time at peak maximum were not constant over the full concentration range [1]. To validate this approach experimentally, the PQ mobility was calculated using the AP as an internal mobility standard. The mobility of AP at 298 K was corrected [14] from that measured at 20–50 m*M*, the ionic strength of the experiment, giving $\mu_{AP}=(3.29\pm0.01)\times10^{-8}$ $m^2\ V^{-1}\ s^{-1}$. Using a_1, μ for PQ was found to be the same within experimental error over the full concentration range 1.2 μ*M*–120 m*M*. Values are (5.13 ± 0.02), (5.13 ± 0.03) and $(5.17\pm0.05)\times10^{-8}$ $m^2\ V^{-1}\ s^{-1}$ with the Gaussian, HVL and triangular functions, respectively. In contrast, when using the peak maximum, whilst no significant difference was found in the ranges where the Gaussian and HVL functions were used [$\mu=(5.13\pm0.02)$ and $(5.09\pm0.04)\times10^{-8}$ $m^2\ V^{-1}\ s^{-1}$], at higher concentrations (4–120 m*M*) when using the peak maximum, the mobility is underestimated by more than 5% [$\mu=(4.97\pm0.04)\times10^{-8}$ $m^2\ V^{-1}\ s^{-1}$].

Figs. 7 and 8 show a_3 as a function of the term $c^{I}_{PQ}l_0$, where c^{I}_{PQ} is the injected concentration of PQ and its product with injection length l_0 is proportional to the amount of paraquat loaded. Fig. 7 covers the concentration range where the HVL function was used for peak fitting (from 120 μ*M* to 4 m*M*), whilst Fig. 8 covers the range where the triangular function was used (from 4 to 120 m*M*). Very good linearity is obtained in both cases. The slope of a_3 as a function of $c^{I}_{PQ}l_0$ was found to be $-(7.57\pm0.04)\times10^{-3}$ $m^3\ mol^{-1}$ with HVL fitting and $-(7.59\pm0.07)\times10^{-3}$ $m^3\ mol^{-1}$ with triangular fitting. In other graphs (not shown), the slopes of normalised area as a function of the term $c^{I}_{PQ}l_0$ were also in very good agreement: $(2.88\pm0.09)\times10^{-1}$ AU $m^2\ mol^{-1}$ with HVL fitting and $(2.87\pm0.09)\times10^{-1}$ AU $m^2\ mol^{-1}$ with triangular fitting, respectively.

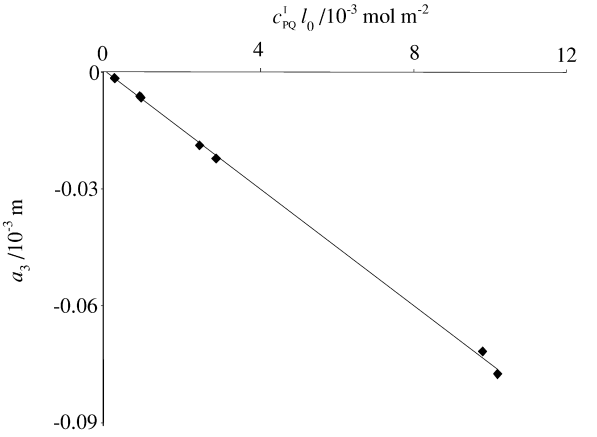

Fig. 7. Sample loading dependence of a_3 extracted from the HVL function for the paraquat peak.

In the measure of peak distortion as a function of loading, there is very good consistency between the HVL and the triangular fitting over the ranges for which they are applicable. As in the results obtained with aminopyridine and discussed in Section 3.2, this

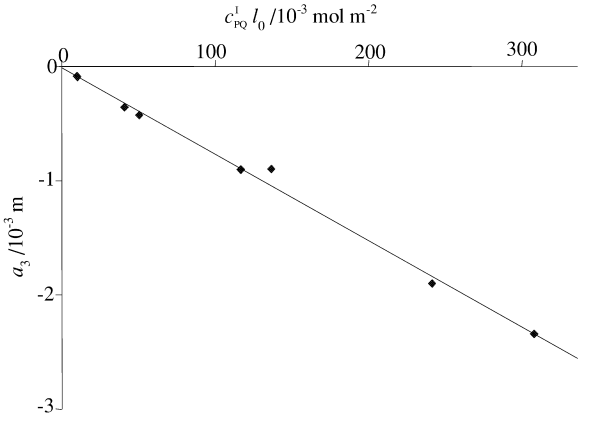

Fig. 8. Sample loading dependence of a_3 extracted from the triangular function for the paraquat peak.

proves the validity of the HVL function for modelling the mix between a Gaussian and a triangular function which is characteristic of CZE peaks. Both the HVL and the triangular function can be used to extract a very good estimation of the A_A coefficient. For the PQ peak, the A_A coefficient is equal to 1.84 ± 0.07 dm^3 mol^{-1}. Unlike the case of AP, the PQ mobility cannot be extracted simply from this coefficient. This is because Eq. (5) from Mikkers theory applies only to systems where there is charge matching between analyte and co-ion. Both AP and its co-ion sodium have charge $1+$, whereas PQ has charge $2+$.

The PQ diffusion coefficient was estimated using Eq. (14) with its mobility corrected to 306 K and zero ionic strength using the formulae of Li et al. for multi-charged analytes [19]. Values at 306 K were found to be $\mu^0_{PQ} = (7.58 \pm 0.05) \times 10^{-8}$ m^2 V^{-1} s^{-1} and $D^0_{PQ} = (1.00 \pm 0.01) \times 10^{-9}$ m^2 s^{-1}. The value of the diffusion coefficient measured at the temperature of the experiment using the observed symmetric peak variance and Eq. (3) was $D^0_{PQ} = (1.09 \pm 0.03) \times 10^{-9}$ m^2 s^{-1}. As for AP, good agreement is found between the theoretical and experimental values.

Excluding values at the lowest concentration (1.2 μM) because of signal-to-noise considerations, as discussed previously, the last two columns in Table 2 show that efficiency stays, within experimental error, constant with value 24×10^4 from $G = 100$ to 91%. N then decreases for values of $G = 71\%$ ($N = 21 \times 10^4$) and below. This validates the conclusion of our previous paper that the distortion due to EMD will not significantly spoil the efficiency unless its variance contribution is greater than one-third of the Gaussian variance (i.e. $G \leq 75\%$) [1]. The paraquat concentration at which EMD will give rise to a 10% reduction in efficiency can be estimated by plotting $1/G$ as a function of concentration. Good linearity was found over the PQ concentration range from 40 μM to 1.2 mM. The PQ concentration corresponding to $1/G = 1/75 = 0.0133$ was found equal to 0.33 mM in the sodium acetate/acetic acid BGE used, with counter-ion concentration 50 mM. The normal rule of thumb for avoiding effects of EMD is to have an analyte/BGE co-ion concentration ratio of 0.01 or less, and this qualitative rule is seen to be in good agreement with our quantitative observations. However, as Mikkers theory (Eqs. (4) and (5)) and Figs. 6–8 show, the key factor for EMD is in fact the product of the analyte/co-ion concentration ratio and the injection length.

4. Conclusion

The HVL function has been shown experimentally to give an excellent description of CZE peak behaviour under conditions where contributions to peak variance from diffusion and electromigration dispersion are comparable. The Gaussian peak centre (a_1) and the standard deviation (a_2) extracted by two fitting functions (Gaussian and HVL) were shown to be constant, independent of the degree of peak distortion. The distortion parameter (a_3) extracted from the HVL and the triangular functions was found to scale linearly with sample loading, as predicted by theory on EMD. For paraquat, this behaviour was demonstrated over a range in concentration of three orders of magnitude. For the 4-aminopyridinium ion, which has the same charge as the BGE co-ion sodium, the analyte mobility calculated from the distortion coefficient is in good agreement with the value measured independently. For both AP and PQ, the diffusion coefficients obtained from experimental data for the symmetric peak variance (a_2) were found to be in good agreement with their theoretical values. These results validate use of the HVL function, and suggest that the theory and fitting functions should be incorporated into routine CZE software in order to improve accuracy of peak analysis and extraction of electrophoretic parameters. Further theoretical work needs to be carried out to adapt Mikkers theory to cases where analyte and BGE co-ions have different charges, as in the case of paraquat and sodium ion, and to cases where there are distributions over several forms of BGE co-ion and/or analyte species.

Acknowledgements

Support from the University of York and Pfizer Global Research and Development for a graduate research studentship for G.L.E. is gratefully acknowledged.

References

[1] G.L. Erny, E.T. Bergström, D.M. Goodall, S. Grieb, Anal. Chem. 73 (2001) 4862.
[2] P.H. Haarhoff, H.J. Van der Linde, Anal. Chem. 38 (1966) 573.
[3] R.A. Mosher, D.A. Saville, W. Thormann, The Dynamics of Electrophoresis, VCH, Weinheim, 1992.
[4] E. Kenndler, in: M.G. Khaledi (Ed.), High-Performance Capillary Electrophoresis; Theory, Techniques and Application, Wiley, New York, 1998, p. 25.
[5] F.E.P. Mikkers, F.M. Everaerts, Th.P.E.M. Verheggen, J. Chromatogr. 169 (1979) 1.
[6] F.E.P. Mikkers, Anal. Chem. 71 (1999) 522.
[7] J.P. Foley, J.G. Dorsey, Anal. Chem. 55 (1983) 730.
[8] A. Klinkenberg, in: R.P.W. Scott (Ed.), Gas Chromatography, Butterworth, London, 1960.
[9] E.T. Bergström, D.M. Goodall, N.M. Allinson, B. Pokric, Anal. Chem. 71 (1999) 4376.
[10] B. Pokric, N.M. Allinson, E.T. Bergström, D.M. Goodall, J. Chromatogr. A 833 (1999) 231.
[11] A. Vinther, H. Soeberg, J. Chromatogr. 557 (1991) 3.
[12] E.T. Bergström, D.M. Goodall, B. Pokric, N.M. Allinson, P.C. Navarro, M.R. Duffin, M.S. Lant, Anal. Chem. (2002) in press.
[13] J. Pospichal, P. Gebauer, P. Bocek, Chem. Rev. 89 (1989) 419.
[14] M.A. Survay, D.M. Goodall, S.A.C. Wren, R.C. Rowe, J. Chromatogr. A 741 (1996) 99.
[15] J. Muzikar, T. Van de Goor, E. Kenndler, Anal. Chem. 74 (2002) 434.
[16] J.M. Knox, Chromatographia 26 (1988) 329.
[17] R.F. Cross, J. Cao, J. Chromatogr. A 809 (1998) 159.
[18] R.C. Weast (Ed.), CRC Handbook of Chemistry and Physics, CRC Press, Boca Raton, FL, 80th ed., 1999–2000, p. 6-3.
[19] D. Li, S.L. Fu, C.A. Lucy, Anal. Chem. 71 (1999) 687.